Flexible non-volatile optical memory TFT device with an unprecedented number of distinct levels based on an organic bi-component blend

Tim Leydecker,[1] Martin Herder,[2] Egon Pavlica,[3] Gvido Bratina,[3] Stefan Hecht,[2*] Emanuele Orgiu,[1*] Paolo Samorì[1*]

[1]*ISIS & icFRC, University of Strasbourg & CNRS, 8 allée Gaspard Monge, 67000 Strasbourg, France.*

[2]*Department of Chemistry & IRIS Adlershof, Humboldt-Universität zu Berlin, Brook-Taylor-Straße 2, 12489 Berlin, Germany.*

[3] *Laboratory for Organic Matter Physics, University of Nova Gorica, Vipavska 13, SI-5000 Nova Gorica, Slovenia.*

Emails: samori@unistra.fr, orgiu@unistra.fr, sh@chemie.hu-berlin.de

Abstract

Organic nanomaterials are attracting a great interest for flexible electronic applications, including logic circuits, displays, and solar cells. While these aforementioned technologies have already demonstrated good performances, flexible organic memories are still to deliver on all their promises in terms of volatility, operation voltages, write/erase speed as well as number of distinct attainable levels. Here, we report on a multilevel non-volatile flexible optical memory thin-film transistor based on a blend of a reference polymer semiconductor, namely poly(3-hexylthiophene), and a photochromic diarylethene, switched with UV and green light irradiation. A three-terminal device featuring over 256 (8 bits storage) distinct current-levels was fabricated, whose memory states could be switched upon 3-ns laser pulses. Furthermore, robustness over 70 write-erase cycles and non-volatility exceeding 500 days are reported. The device was implemented on a flexible PET substrate, validating the concept for integration into wearable electronics and smart nanodevices.

INTRODUCTION

While silicon-based technology is still effectively leading today's electronic industry, the development of high-performance organic semiconducting nanomaterials has been the topic of important research efforts in the past two decades. [1-3] Such materials unambiguously represent an interesting alternative since their properties can readily be tuned via *ad-hoc* chemical synthesis and they allow for mild processing from solution using approaches, which can be up-scaled and applied to "soft" substrates, thereby making them ideal candidates for the low-cost fabrication of large-area electronic devices. These materials have shown exceptional versatility, enabling integration on flexible and/or transparent substrates for a new generation of electronics. [4-7] Among the plethora of applications of semiconducting organic materials and more generally of π-conjugated (macro)molecules, memories have attracted a special interest because they combine high switching ratios, [8-10] and long retention times [11] as well as low operating voltages [12-14] and the possibility to be integrated onto flexible substrates. [15-18]

In order to increase data storage capabilities in electronic devices (i.e. hard drives, random access memories, etc.), the most popular approaches thus far rely on the continuous scaling down to enable integration of an increasing number of memory cells per area unit. These strategies have shown their limits, as scaling down is hampered by photolithography while fabrication complexity has increased dramatically over the years.[19,20] An alternative method is based on the development of memory cells with increased storage capabilities for multilevel memories. In the case of 1-bit storage devices, a finite yet limited degree of volatility is not detrimental to the overall storage capacity as long as the two states, typically represented by a current maximum and minimum, are still distinguishable. The main challenge is to obtain the highest possible difference in current between an "on-state" and an "off-state". When multilevel memories are considered, the conundrum shifts dramatically to the stability of states, as each state will necessarily be close to others. In the example of a 4-bit memory cell (16 current levels), one order of magnitude difference between each level is unachievable, since this would mean a switching ratio as high as 10^{15}. Importantly, all those methods where a high switching ratio is simply based on a threshold voltage shift (i.e. not characterized by a change in charge carrier mobility or current) with the "read voltage" within the threshold voltage window are prone to data loss and incorrect reading of the levels in multilevel storage. [21,22]

2-Terminal and 3-terminal resistive switching memories based on polymers, organic small molecules and ferroelectric materials have shown impressive switching ratios up to 10^8 and low programming voltages. [23-25] Unfortunately, this approach relies on two stable states of polarization therefore it is ill suited for multilevel memories. [26] On the other hand, memories designed around electrets, i.e. dielectric materials (usually polymers), or using polymer/electrolyte pairs exhibiting

quasi-permanent electric charge or dipole polarization, have displayed ability to perform as multilevel memories with different applied programming voltages. Although the observed switching ratios over 10^8 push them at the forefront of research on organic memories, [27-30] their unacceptably high programming voltages (up to ± 200 V) and most importantly their low retention times ($<10^4$ s) represent still major obstacles towards their integration into everyday electronics. [31,32] Storing charges in a metal or semiconductor layer exploiting the principle of the floating gate located within the dielectric can be achieved with metallic nanoparticles, with each particle counting as a charge-storage site independent and isolated from other sites. While not extensively explored, this approach is relevant for the fabrication of multilevel memories exhibiting acceptable programming voltages (up to ± 40 V) but thus far is accompanied by disappointing retention times for long-term multilevel storage (10^4 s). [33]

As compared to electrical programming of organic memories, photoprogramming offers the fundamental advantage of having the photowriting being orthogonal to the electrical readout. Photochromic molecules have shown promising results as molecular switches, but rather mediocre (semi)conducting behavior and not negligible fatigue. [34-36] Most studies on organic memories based on photochromic molecules have focused on three types of photochromic systems: azobenzenes, spiropyrans, and diarylethenes (DAEs). [37-40] Optical switching between two independently addressable states leads to changes both at the molecular and at the macroscopic scale. At the molecular level, one observes reversible modifications of the geometrical and electronic structure, including changes in dipole moment, π-conjugation, band-gap, etc.,[41] which can be translated into respective adaptations of macroscopic properties upon switching, including changes in shape, aggregation behavior and conductance. While conductance changes are often a sought-after property, concomitant morphological changes at the meso-scale could lead to stability issues, in particular since maintaining high order in the film is crucial for device performance. Therefore, the optimal solution consists of a photochromic molecule in which the two switching states exhibit simultaneously (i) the lowest possible change in supramolecular organization, (ii) the largest modulation of the electronic properties, (iii) sufficient stability of both interconverting isomers, (iv) a fast switching induced by the light stimulus, and (v) an efficient switching in the solid state. All of these characteristics can be met by DAEs. [42] In earlier studies, organic memories based on layered device architectures composed of DAE and triarylamine derivatives proved to be a valuable approach for the production of organic multilevel memories with 30 reported current-levels. [43,44] However, the fabrication of multi-layers clearly requires multi-step processing, and the devices need several minutes of irradiation at high intensity in order to obtain a sufficient switching yield, making them unsuitable for applications in the electronic industry. Furthermore, electrical switching exhibited a limited reversibility, retention time and storage capacity, thereby hampering any technological applications in memory devices. Another grand

challenge is the implementation of such devices on flexible substrate, in the perspective of foldable smart electronics.

Here we use bi-functional organic thin-film transistors with an active layer consisting of a blend of a DAE moiety, namely DAE-Me (Figure 1a), with a reference semiconducting polymer such as poly(3-hexylthiophene) (P3HT) serving as the electroactive nanomaterial. The dual functionality in our devices relies on the large photoinduced modulation of the energy levels of the DAE-Me photoswitch in the polymer matrix that allow optical control over charge transport. When the DAE-Me is in its open form (DAE-Me_o) the corresponding HOMO level lies outside of the P3HT's bandgap therefore simply acting as a scattering center for charge carriers. However, the closed isomer (DAE-Me_c) features a HOMO level, which is situated within the band gap of the polymer matrix and can therefore accept holes. This principle of photoswitchable charge trapping has already been proven in an earlier seminal study and recently extended to both p- and n-type small molecules. [45-47] These works served as proof of principle experiments that provided evidence for the basic mechanisms of interaction between DAEs and P3HT. Essentially, these fundamental works revealed that when energy levels of the components are properly engineered the DAEs act as hole-accepting levels within the matrix of a polymer semiconductor. As a result, the insertion of DAE-Me within a P3HT matrix offers a remote control of the output drain current in an OTFT by light.

In the present work we present a three-terminal memory device where the active layer is composed of an organic bi-component DAE/P3HT thin film. We show that such a combination of nanomaterials can be successfully used in real technological applications to fabricate non-volatile organic-based memories with high density of information storage. The choice of a three-terminal transistor device geometry as a memory element[47] was made due to its superior technological relevance over diode (two-terminal) devices. Transistors are able to implement a signal addressing function in two-dimensional memory arrays that would not be possible if diode-only circuits are employed. Significantly, these memory devices can be supported onto flexible substrates: upon 1000 bending cycles, the current measurements revealed no particular changes neither for the device with diarylethenes in the open form nor for the device with diarylethenes in the closed form, proving excellent data retention characteristics.

By virtue of the photochromic DAE molecules dispersed in the polymer matrix and acting as hole traps, the rate of charge carriers collected at the drain electrode over time can be precisely tuned by the light intensity and duration at specific wavelengths. This irradiation dose dictates the population of the open vs. closed DAE isomers in the blend therefore allowing to exactly control the device output current. In this setup we can realize a cognitive device, in which light irradiation triggers the *learning* process and the stability of the particular bit of information is ensured by the long retention times of the molecular DAE system.

RESULTS AND DISCUSSION

Three-terminal memory devices on SiO_2

We first explored bottom-gate bottom-contact field-effect transistors using a SiO_2 layer as the gate dielectric (Figure 1a). The bi-component active layer comprising the photochromic DAE moiety in a P3HT polymer matrix was spin-coated from a solution in chloroform and then electrically characterized in a nitrogen-saturated atmosphere of a glove box. Furthermore, we have tested several combinations of p-type matrices other than P3HT, such as polyfluorene- and isoindigo-based polymers, but found that the quantum yield of the isomerization reaction was poor if compared to that obtained in P3HT (data not shown here). In order to confer a high starting crystallinity to the polymer active layer and enhance its electrical performances, octadecyltrichlorosilane (OTS) chemisorbed self-assembled monolayers were formed on the SiO_2 dielectric surface.[48] OTS treated devices featured smooth DAE-Me/P3HT films with a root-mean-square roughness (R_{RMS}) of 0.54 nm, reduced from 0.74 nm R_{RMS} of films supported on pristine silicon oxide (calculated from Atomic Force Microscopy data plots presented in the SI at Section 5). Films on OTS treated silicon oxide resulted in increased currents exceeding one order of magnitude. Transfer curves (I_{DS}-V_{GS}) were used to quantify the devices' field-effect mobility (μ_{FET}), threshold voltage (V_{th}), and I_{on}/I_{off}. Exemplary output curves are reported in the supplementary information (SI). The electrical characterization revealed devices featuring classical p-type transfer characteristics and high field-effect mobilities for P3HT (0.01 $cm^2V^{-1}s^{-1}$, see Section 2 of the SI). The current ratio measured in the active layer comprising the photochromic unit either in the open or the closed form ("switching ratio") was extracted from the I_{DS}-V_{GS} curves. In particular, the I_{DS} was measured in the dark once the diarylethene isomer in the bi-component film is turned into its open (DAE-Me_o) or in majority into its closed (DAE-Me_c) isomer upon irradiation with monochromatic light at λ = 546 nm (*erase*) or 313 nm (*write*), respectively. To better compare our results with the scientific literature, we employed the ratio $I_{DS,DAE\text{-}Me\_o}$ /$I_{DS,DAE\text{-}Me\_c}$ (measured at the same V_{DS} and V_{GS}) as a figure of merit. As evident from Fig. 1b the threshold voltage shifts towards negative bias (ΔV_{th} amounting to ca. to -15 V) was observed when the DAE molecules were converted from their open to their closed isomer. The resulting difference in threshold voltage between the open and closed forms enables a switching ratio over 10^5 for V_{th} (open form) < V_{GS} < V_{th} (closed form) (Figure 1c). Nevertheless, contrary to single level memories, their multilevel counterparts require fine-tuning of each current-level. Therefore, in order to increase the reliability of the device, the "dynamic range" between the extreme off and on levels ($I_{DS,DAE\text{-}Me\_o}$ - $I_{DS,DAE\text{-}Me\_c}$ at a fixed V_{DS} and V_{GS}) should be maximized. Hence, further measurements have been performed at V_{GS} = - 60 V.

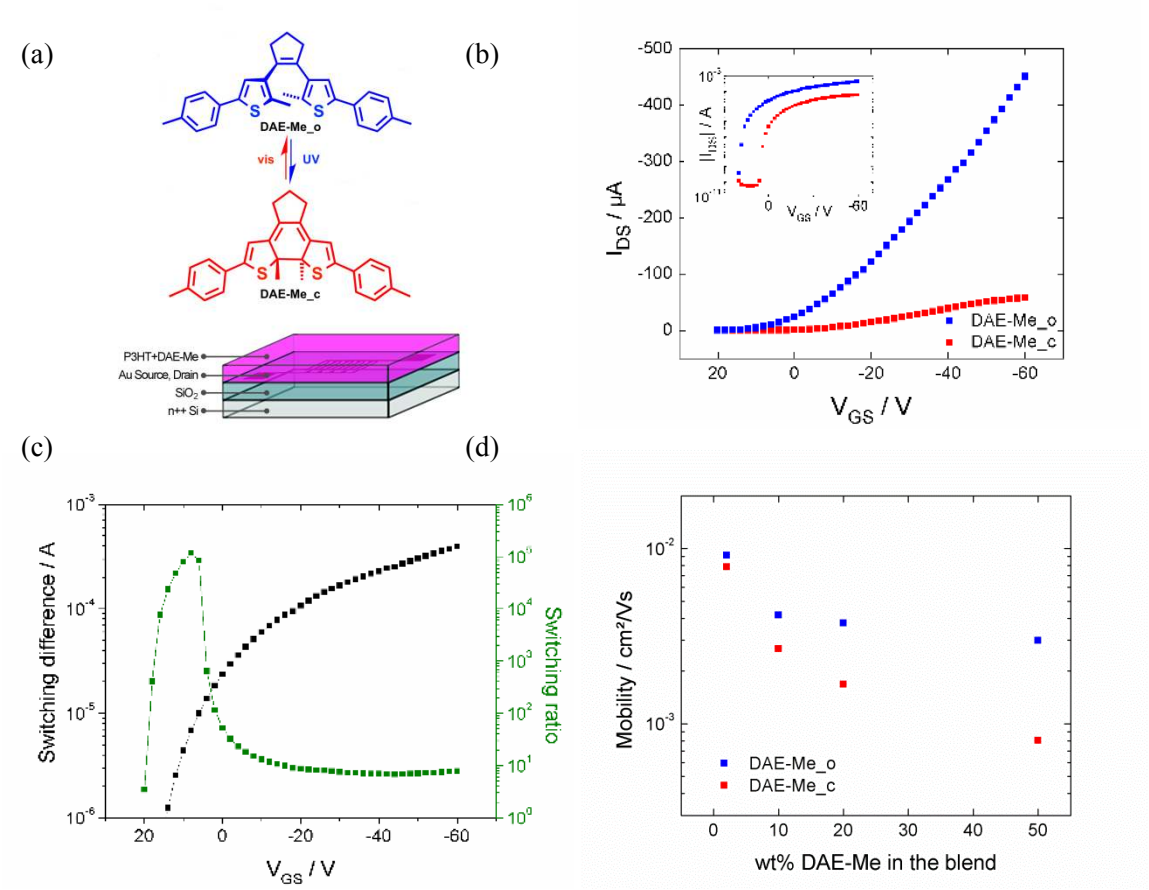

Figure 1: Electrical characterization of the bottom-gate/bottom contact P3HT/DAE-Me devices. (a) Chemical formulae of the employed diarylethene in its open and closed form, bottom: structure of the devices on SiO_2 substrate; (b) I_{DS}-V_{GS} in the open and the closed form (after 10 minutes of irradiation at λ = 313 nm), at V_{DS} = - 60 V. In the inset, the same curve is represented in logarithmic scale; (c) switching ratio ($I_{DS,DAE\text{-}Me\_o}/I_{DS,DAE\text{-}Me\_c}$) and switching difference ($I_{DS,DAE\text{-}Me\_o}$ - $I_{DS,DAE\text{-}Me\_c}$) as a function of the gate voltage; (d) average μ_{FET} of the devices as a function of the weight percentage of diarylethenes in the blend.

Different amounts of DAE added to P3HT (wt%) were tested in order to explore the effect of the mutual ratio on the electrical performances and switching capabilities (Figure 1d). We have found that mobilities decreased when the amount of DAE in the blend was increased (both in open and closed form). Therefore, the highest mobilities were found at 2 wt% DAE-Me in the blend, with a small yet significant 15% decrease in mobility upon irradiation with UV light. The amplitude of the light-induced switching process (in terms of μ_{FET}) of the devices was improved when a superior amount of DAE was introduced in the blend spin-coated onto the device. As mentioned above, while a high switching ratio is preferable (as was obtained with DAE-Me and P3HT blended in equivalent amounts), it is crucial to preserve high electrical performances to achieve multilevel storage with a high number of distinguishable current levels. A good compromise between mobility and switching

ratio was found with 20 wt% DAE in the blend. The difference in device threshold voltage between open and closed form remained constant ($\Delta V_{th} = V_{th[DAE\text{-}Me\_o]} - V_{th[DAE\text{-}Me\_c]} \sim +15$ V) upon increasing quantities of DAE-Me in the blend (values are represented in the supporting information, Figure S3a). This difference can be ascribed to the change in the number of trapped charges between open and closed form owing to the presence of the hole-accepting levels featured by the DAE-Me in the closed form. Furthermore, a general threshold voltage shift can be observed upon addition of DAE-Me for both forms. While DAE-Me in its open form can only act as a scattering center for charges, its presence will occupy an increasing effective area in the channel with increasing the wt%. The associated reduction of the crystalline portions of the film will then give rise to such shift. Regarding DAE-Me in its closed form, the increasing threshold voltage stems from the increased amount of charge trapping sites within the film.

As long as the quantum isomerization yield of the photochromic component is high enough within a given matrix, our blending approach is versatile as it allows for tailoring to any desired DAE/polymer pair depending on the application at hand and the materials in use, [34,45-47] contrary to the separate layer approach that is typically used in the context of organic two- and three-terminal memories. [43,44]

The endurance of the semiconductor-DAE blend was tested by dynamic write-erase cycles at constant bias. On this occurrence and throughout the entire manuscript, continuous measurement of the I_{DS} current as a function of time will be referred to as dynamic characterization. In order to determine the sole contribution of the DAE to the I_{DS} current change, the decay observed due to bias stress on P3HT was estimated from the curve before illumination, and deduced from the I_{DS}-time plot. Additional explanations and fitting parameters are given in the SI, Section 3. On over 70 write-erase cycles (10 s cycles after 20 min of measurement without illumination), the switching fatigue was found to be negligible. This is a good indication for the stability of the devices as they can undergo a large number of write-erase cycles with minor impact on their switching ability (Figure 2a and 2b). The retention capabilities of the devices have been tested by measuring the I_{DS} current at a fixed V_{DS} of - 10 V and V_{GS} of - 60 V in the open and the closed form after different storage times in the dark. No modification of the currents was found after 64 days in the dark, providing clear evidence for excellent retention capabilities reaching 500 days (Figure 2c).

Read-out accuracy of the memory was evaluated through current measurements in the dark upon switching cycles performed with a monochromator setup (Figure 2d). Each of the current levels 1, 2, 3, and 4 was reached with a different irradiation time at 313 nm, while the level 0 was recovered by irradiation at 546 nm. The standard deviation was calculated for each level and compared to the total current difference between the memory with the diarylethenes in the open form and the memory with the diarylethenes in the closed form (values reported in Table T3 the SI). For each level, the

standard deviation was below 0.5% of the total gap (80 µA), demonstrating excellent read-out accuracy.

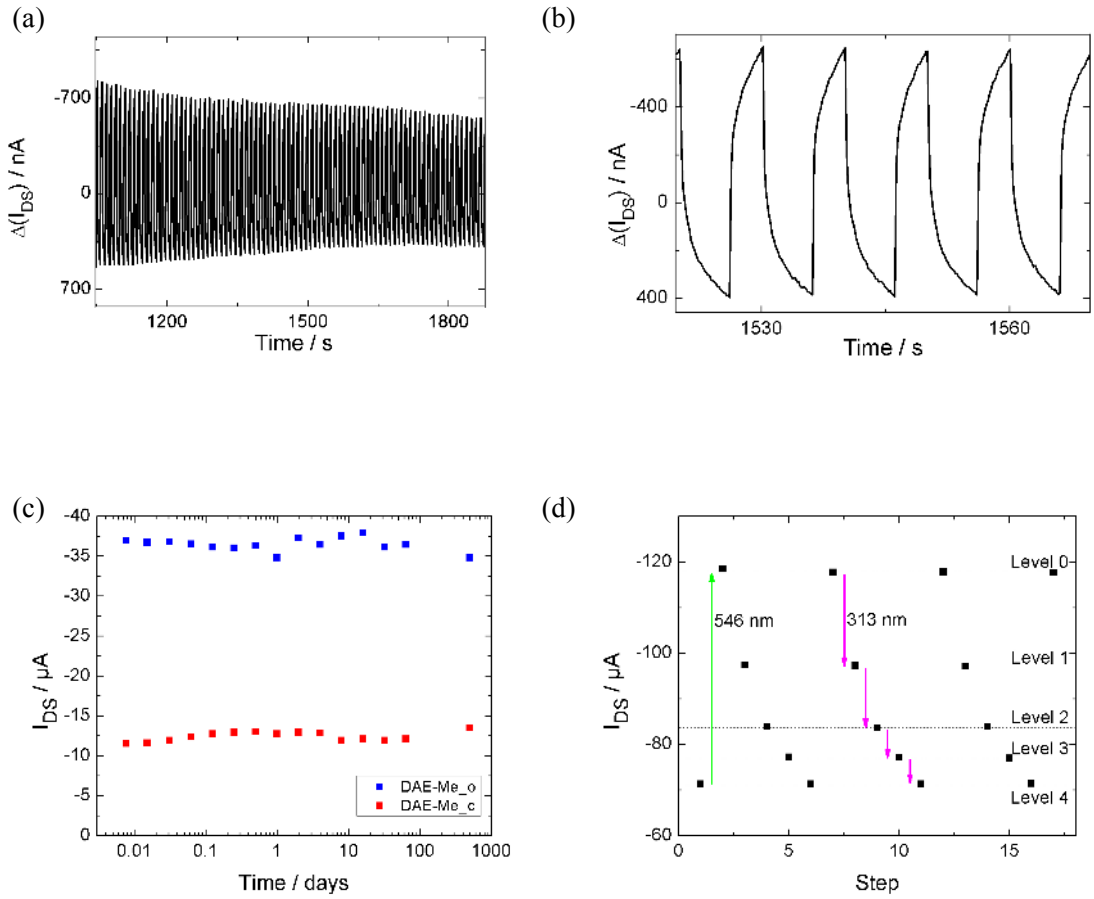

Figure 2: Data retention of the memory device. (a) and (b) Experimental dynamic I_{DS}-time curves, corrected for bias stress, at V_{DS} = -10 V and V_{GS} = -60 V: writing for 1 second at 313 nm and erasing for 5 seconds at 546 nm. 70 cycles are shown in (a) while only 5 of them are to be seen in (b). ΔI_{DS} is defined by $\Delta I_{DS} = I_{DS} - I_{DS,t(initial)}$; (c) measurement of the I_{DS} current after different times of storage of the device in the dark at fixed V_{DS} = -10 V and V_{GS} = -60 V to illustrate the retention capability of the devices in the open and the closed form; (d) Static switching cycles at fixed illumination times. The current was measured for a single point in the dark at V_{GS} = -40 V and V_{DS} = -10 V. Level 0 → Level 1: 10 s at 313 nm, Level 1 → Level 2: 20 s at 313 nm, Level 2 → Level 3: 30 s at 313 nm, Level 3 → Level 4: 60 s at 313 nm, Level 4 → Level 0: 615 s at 546 nm.

Switching with ultrafast light irradiation

A laser-setup with ultra short time pulses was used in order to investigate the photo-induced switching upon illumination times associated with modern optics and electronics. The device was exposed to a 3 ns laser pulse (λ = 313 nm) at tunable intensity in intervals of ten seconds leading to a progressive current decrease controlled by the number of pulses. Each pulse generated a ΔI_{DS} step decrease owing to the increasing amount of photogenerated hole traps, i.e. DAE-Me_c. Each current step has a certain height and this allowed us to estimate the *signal-to-noise* ratio (SNR) calculated from the RMS amplitude of the noise over 3×80 consecutive points (see SI, Section 6). Within the first current levels SNR exceeds 50, and decreases to 2.8 in the final steps. The decrease results from the graduate reduction of the step height with a noise value that remains constant. We have successfully built a 400 current-intensity level device (Figure 3), reaching a data storage capacity over 8 bit (256 levels). By reduction of the light intensity using filters, we have shown that the step in height is dependent on the areal power density (see SI, Section 4) because the number of molecules undergoing photoisomerization is proportional to the density of the photons hitting the device area. In particular, our device can already operate at incident power < 1 μJ $cm^{-2}s^{-1}$. The number of steps and hence the storage density is therefore only limited by the noise in the signal (leading to a maximum of 5000 steps in the presented experiment) with a theoretical maximum given by the number of steps equal to the number of DAE molecules in the channel.

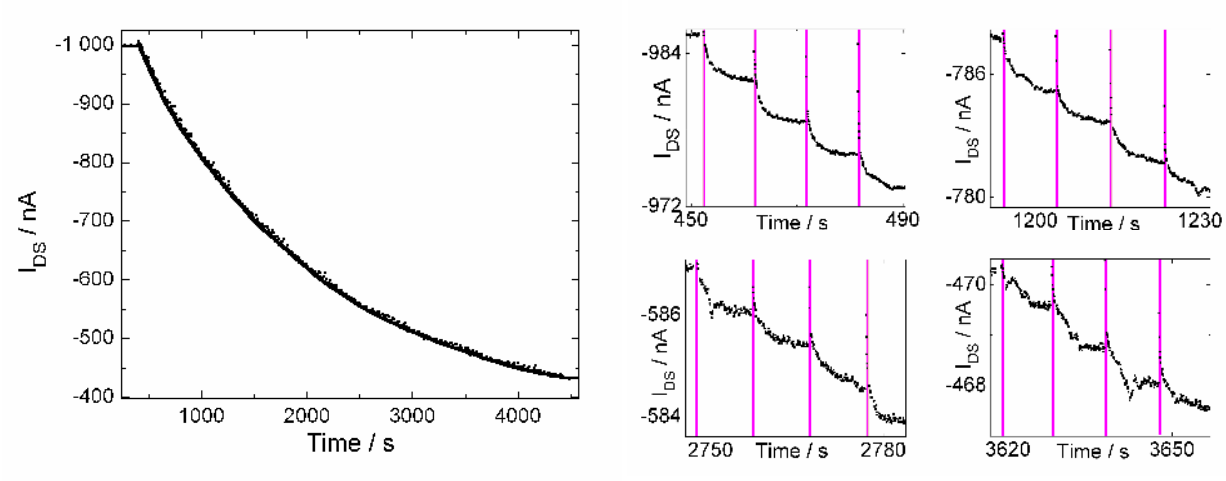

Figure 3: I_{DS}-time curves (corrected for bias stress) under irradiation of the device with 3 ns laser pulses (313 nm) every 10 s, underlining the ability to behave as a multilevel memory. Curves were plotted at V_{GS} = -60V and V_{DS} = -10V. Current-spikes in the curve are attributed to photo-generated carriers during irradiation. Given their short duration (3 ns) illumination steps are not represented to scale.

Three-terminal device memories on a flexible PET substrate

In view of the ultimate goal of demonstrating the possible implementation of the memory-devices into novel electronic applications, the whole procedure (apart from OTS treatment) was transferred to a flexible substrate, trading the rigid inorganic silicon based layers for polymeric sheets of polyethylene terephthalate (PET), poly(methyl methacrylate) (PMMA) and poly(4-vinylphenol) (PVP) (Figure 4a). The bottom gate configuration was selected again to benefit from unfiltered irradiation of the active layer. While the PMMA dielectric ensured low current leakage, the PVP layer deposited on top made spin-coating of the chloroform-based solution possible. The devices were electrically characterized and the field-effect mobilities were comparable to those on SiO_2 without OTS (over 10^{-3} $cm^2V^{-1}s^{-1}$). Switching capabilities were tested over multiple dynamic switching cycles. We have found that the devices could be switched between closed and open states, albeit at slower pace when compared to devices on SiO_2 (Figure 4b). The small increases of drain current during switching are attributed to photogenerated carriers. Dynamic I_{DS}-time curves with small illumination steps at 313 nm indicate the ability of the device to work as a 4-bit multilevel memory (16 distinct levels, Figure 4c). Furthermore, electrical characterization was performed on the device after successive bending cycles (Figure 4d). Upon 1000 cycles, the current measurements revealed no particular changes neither for the device with diarylethenes in the open form nor for the device with diarylethenes in the closed form. Longer bending steps at different bending radii (amounting to 29.0 mm, 17.5 mm, 10.0 mm, 8.0 mm, and 6.0 mm) were performed. Post-bending performances were still comparable to those observed before bending at each bending radius for 60 seconds (Figure S5), with only minor losses in terms of charge carrier mobility and a slight shift in the threshold voltage, proving that with further optimization, the studied organic 3-terminal memory devices could be introduced into flexible electronics.

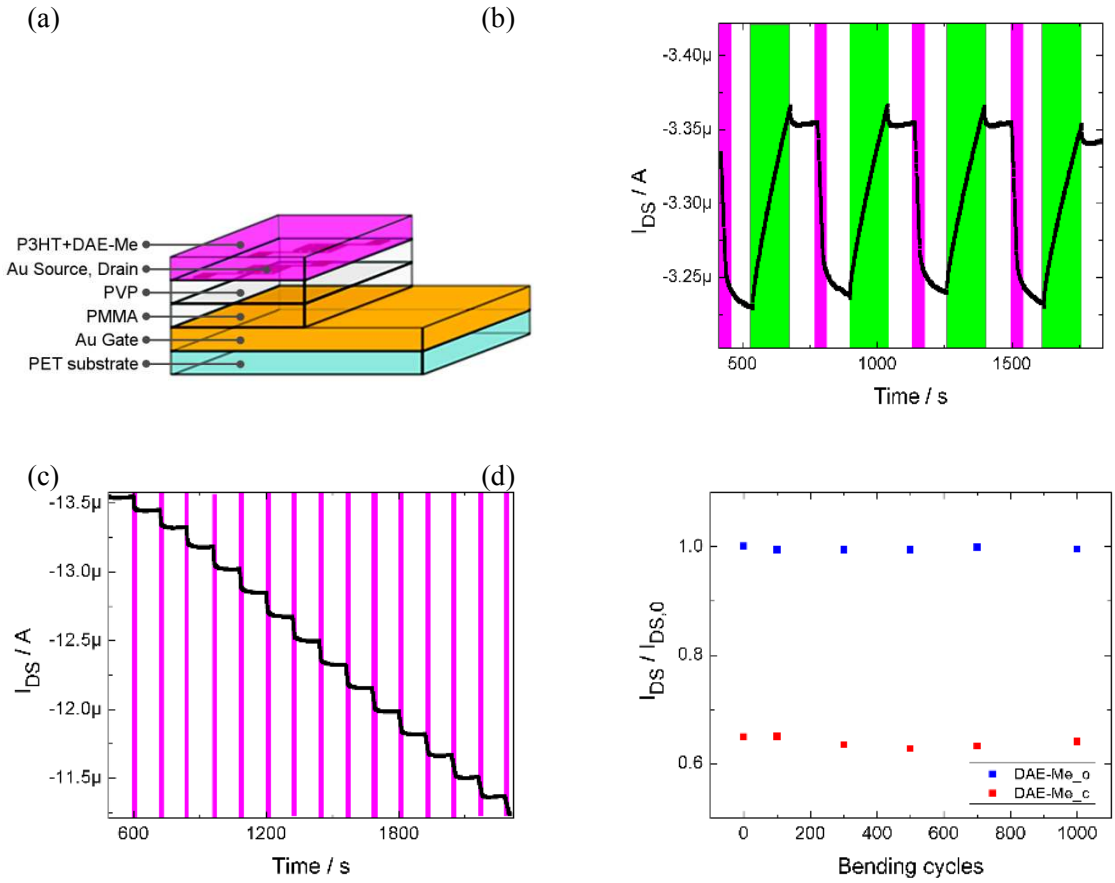

Figure 4: Integration of the memory unit onto a flexible PET substrate. (a) Structure of the devices on PET (top to bottom: DAE/P3HT blend, Au source/drain electrodes, PVP dielectric, PMMA dielectric, Au gate electrode and PET substrate); (b) Experimental dynamic I_{DS}-time curves, corrected for bias stress, with write-erase cycles (313 nm for 20 s /546 nm for 140 s) at V_{GS} = - 60 V and V_{DS} = - 10 V; (c) I_{DS}-time curve corrected for bias stress showing small irradiation steps at 313 nm underlining the ability to behave as a multilevel memory (5 to 20 seconds incremental irradiation steps); (d) Drain current as a function of bending cycles involving samples devices based on either diarylethenes in the closed form (after 10 min irradiation at 313 nm) or in the open form. Each cycle consisted of 5 s of bending at a bending radius of 8.0 mm, followed by 5 s of resting time.

CONCLUSIONS

We have shown that it is possible to build 3-terminal memory-devices with unprecedented features. Above all, the ability to define many distinct current levels paves the way for high-density memories with 8-bit memory units (256 levels). Illumination times using a laser setup are on the nanosecond time scale, giving rise to a fast response that is necessary for real-life electronics. It has been shown

that this approach can be successfully applied also on flexible substrates. Furthermore, the excellent data retention capabilities of the devices (retention times of 10^7 s) and the reliability after many write-erase cycles make this method ideal for the future applications in (flexible) electronics. Due to the versatile nature of our blending approach, the air-sensitive P3HT could be replaced by an alternative air-stable p-type semiconductor with similar energy levels, leading to potentially higher currents (hence an increased possible number of steps) without the need for encapsulation. Alternative polymer/DAE pairs should be selected in accordance to their respective energy levels, ideally placing the HOMO level of the closed DAE as deep as possible within the bandgap of the polymer while the HOMO level of the open DAE should be outside of the bandgap of the polymer. Furthermore, the interplay between small molecule and polymer should be considered carefully in order to avoid aggregation of the DAE. Both the energetic levels and the phase segregation can be tuned by the functionalization of the photochromic units. Moreover, attaining multilevel memory requires the use of a semiconducting (macro)molecule exhibiting mobilities > 10^{-3} $cm^2V^{-1}s^{-1}$ to ensure detectable photomodulated change in the device current after hundreds of cycles. Furthermore, while in principle the optimal scenario consists of DAE/semiconductor pairs with orthogonal absorption bands, in our case the use of films with a thickness of just few tens of nanometers makes this requirement less stringent even when low irradiation doses are employed.

Our findings are of paramount importance for the realization of a light-controlled cognitive nanodevices where the irradiation history represents the learning process and the non-volatile state retention ensures that the data are preserved over time in a given memory state. The possibility of developing such devices on a flexible substrate and to write using ultra-short low-intensity laser pulses is of paramount importance for the development of high performing optically gated electronic nanodevices for potential applications in memories, logic circuits and more generally in optoelectronics and optical sensing.

METHODS

Memories on SiO_2. Bottom-contact bottom-gate configuration transistors purchased from IPMS Fraunhofer Institute were used. They consisted of on n^{++}-Si substrates with 230 nm of thermally grown SiO_2 as the gate dielectric (15 nF capacitance) and pre-patterned pairs of gold electrodes with interdigitated geometry as the source and drain. All solutions, samples and devices were prepared and measured in a N_2 filled glovebox to avoid oxidative doping of the materials and ensure reproducibility of the experiments. OTS was purchased from Sigma-Aldrich. OTS treatment consisted of a 12-hours immersion of the ozone-treated wafer into a 10 mM solution of OTS in toluene with 30 min of heating at 60 °C at the beginning of the immersion. The samples were afterwards rinsed with toluene and heated for 60 min at 60 °C. Subsequently, 100 µL of the P3HT-DAE-Me_o solution was spin-coated onto the OTS treated wafer at 1500 RPM (acceleration: 4000 $RPM.s^{-1}$). P3HT at 50 kDa (dispersity

2.4) synthesized by BASF (commercialized under the name "Sepiolid P200") was purchased and used as received without further purification. The DAE-Me/P3HT solution consisted of a blend of 0.4 mg of DAE-Me_o and 1.6 mg of P3HT in 1mL of chloroform.

Memories on PET. A square PET film (thickness = 175 μm) was attached to a glass substrate using thermal tape and 60 nm of Au were subsequently evaporated on top of the PET in order to form the gate electrode. One side of the sample was protected from the next steps of the procedure with a small strap of thermal tape. A layer of the dielectric poly(methyl methacrylate) (PMMA) was spin-coated onto the gate electrode, and annealed one hour at 120 °C. An additional dielectric, poly(4-vinylphenol) (PVP) was spin-coated on the PMMA and annealed two hours at 150 °C. The interdigitated gold source and drain electrodes were vacuum-deposited on the dielectric through shadow masks (layer thickness = 60 nm). Finally, the semiconducting P3HT/DAE blend was spin-coated as the final layer of the sample. The DAE-Me_o/P3HT solution consisted of a blend of 0.4 mg of DAE-Me_o and 1.6 mg of P3HT in 1 mL of chloroform.

Device characterization. The device characteristics were measured by contacting the source, drain and gate electrodes and applying different voltages in order to get I_{DS}/V_{GS} graphs. Measurements were all performed using Keithley devices and the software Labtracer. In the case of I_{DS}-V_{GS} graphs (transfer curves) each was made by sweeping the gate voltages from + 40 V to - 60 V, with one measurement every 2 V. The drain voltage was either -10 V (linear regime) or - 60 V (saturation regime). The I_{DS} current was measured each time. Using the software Origin pro 8.0, transfer curves are plotted and fitted in order to extract the value of the mobility and the threshold voltage. Output curves are used to extract the value of the I_{on}/I_{off} ratio, by dividing the value of the observed current at saturation regime when the transistor is "on" (V_{GS} = - 60 V) by the value of the current when the transistor is "off" (V_{GS} = + 40 V).

Experimental data were analyzed using standard field-effect transistor equations (for *p-type* semiconductors) for the saturation regime:

$$I_{DS} = -\frac{W}{2L}\mu C_{TOT}(V_{GS} - V_{Th})^2$$

Mobility of samples with two dielectrics (PVP and PMMA) was calculated using the value of the total capacitance given by $C_{TOT} = (C_{PMMA} \times C_{PVP}) / (C_{PMMA} + C_{PVP})$. The thickness of each layer was measured using a profilometer.

Dynamic switching was observed by tracing of I_{DS}-time curves at constant Gate-Source voltage and constant Drain-Source voltage. The samples were illuminated while being biased and I_{DS}-current was measured. Illumination was performed using either a laser setup (85±17 μJ cm^{-2} for each 3 ns pulse,

memories on SiO_2) or a monochromator setup (74 μJ cm^{-2} per second of irradiation at 313 nm, memories on PET and static switching cycles of memories on SiO_2 substrate).

Acknowledgments

This work was financially supported by EC through the MSCA-ITN project iSwitch (GA no. 642196) as well as the ERC projects SUPRAFUNCTION (GA-257305) and LIGHT4FUNCTION (GA-308117), the Agence Nationale de la Recherche through the LabEx CSC (ANR-10- LABX-0026_CSC), the International Center for Frontier Research in Chemistry (icFRC), and the German Research Foundation (via SFB 658).

Author Contributions

P.S. and E.O. conceived the experiment and designed the study. M.H. and S.H. designed the DAEs and carried out their synthesis and electrochemical characterization. T.L., E.O., G.B. and E.P. designed and performed the time-response measurements. E.O designed and T.L. performed the device experiments. T.L, E.O. and P.S. co-wrote the paper. All authors discussed results and contributed to the interpretation of data as well as contributed to editing the manuscript.

Competing financial interests: The authors declare no competing financial interests.

References

1 Kelley, T. W. *et al.* Recent progress in organic electronics: Materials, devices, and processes. *Chem. Mater.* **16**, 4413-4422 (2004).
2 Braga, D. & Horowitz, G. High-Performance Organic Field-Effect Transistors. *Adv. Mater.* **21**, 1473-1486 (2009).
3 Han, S. T., Zhou, Y. & Roy, V. A. L. Towards the Development of Flexible Non-Volatile Memories. *Adv. Mater.* **25**, 5425-5449 (2013).
4 Benight, S. J., Wang, C., Tok, J. B. H. & Bao, Z. A. Stretchable and self-healing polymers and devices for electronic skin. *Prog. Polym. Sci.* **38**, 1961-1977 (2013).
5 Pang, C., Lee, C. & Suh, K. Y. Recent advances in flexible sensors for wearable and implantable devices. *J. Appl. Polym. Sci.* **130**, 1429-1441 (2013).
6 Baeg, K. J., Caironi, M. & Noh, Y. Y. Toward Printed Integrated Circuits based on Unipolar or Ambipolar Polymer Semiconductors. *Adv. Mater.* **25**, 4210-4244 (2013).

7 Ahmad, S. Organic semiconductors for device applications: current trends and future prospects. *J. Polym. Eng.* **34**, 279-338 (2014).
8 Chiu, Y. C. *et al.* High-Performance Nonvolatile Organic Transistor Memory Devices Using the Electrets of Semiconducting Blends. *ACS Appl. Mater. Inter.* **6**, 12780-12788 (2014).
9 Smithson, C. S., Wu, Y., Wigglesworth, T. & Zhu, S. A More Than Six Orders of Magnitude UV-Responsive Organic Field-Effect Transistor Utilizing a Benzothiophene Semiconductor and Disperse Red 1 for Enhanced Charge Separation. *Adv. Mater.* **27**, 228-233 (2015).
10 Yoon, S. M. *et al.* Fully Transparent Non-volatile Memory Thin-Film Transistors Using an Organic Ferroelectric and Oxide Semiconductor Below 200 degrees C. *Adv. Funct. Mater.* **20**, 921-926 (2010).
11 Radha, B., Sagade, A. A. & Kulkarni, G. U. Metal-organic molecular device for non-volatile memory storage. *Appl. Phys. Lett.* **105** (2014).
12 Liu, X. H. *et al.* The effect of oxygen content on the performance of low-voltage organic phototransistor memory. *Org. Electron.* **15**, 1664-1671 (2014).
13 Nougaret, L. *et al.* Nanoscale Design of Multifunctional Organic Layers for Low-Power High-Density Memory Devices. *ACS Nano* **8**, 3498-3505 (2014).
14 Lee, S. *et al.* Overcoming the "retention vs. voltage" trade-off in nonvolatile organic memory: Ag nanoparticles covered with dipolar self-assembled monolayers as robust charge storage nodes. *Org. Electron.* **14**, 3260-3266 (2013).
15 Kim, S. J. & Lee, J. S. Flexible Organic Transistor Memory Devices. *Nano Lett.* **10**, 2884-2890 (2010).
16 Cosseddu, P., Lai, S., Casula, G., Raffo, L. & Bonfiglio, A. High performance, foldable, organic memories based on ultra-low voltage, thin film transistors. *Org. Electron.* **15**, 3595-3600 (2014).
17 Kim, R. H. *et al.* Non-volatile organic memory with sub-millimetre bending radius. *Nat. Commun.* **5** (2014).
18 Sekitani, T. *et al.* Organic Nonvolatile Memory Transistors for Flexible Sensor Arrays. *Science* **326**, 1516-1519 (2009).
19 Liu, X. *et al.* Advancements in organic nonvolatile memory devices. *Chin. Sci. Bull.* **56**, 3178-3190 (2011).
20 Bez, R., Camerlenghi, E., Modelli, A. & Visconti, A. Introduction to Flash memory. *Proc. IEEE* **91**, 489-502 (2003).
21 Sala, F., Gabrys, R. & Dolecek, L. Dynamic Threshold Schemes for Multi-Level Non-Volatile Memories. *IEEE T. Commun.* **61**, 2624-2634 (2013).
22 Pirovano, A. *et al.* Reliability study of phase-change nonvolatile memories. *IEEE T. Device Mat. Re.* **4**, 422-427 (2004).
23 Nili, H. *et al.* Nanoscale Resistive Switching in Amorphous Perovskite Oxide (a-SrTiO3) Memristors. *Adv. Funct. Mater.* **24**, 6741-6750 (2014).
24 Han, Y., Cho, K., Park, S. & Kim, S. Resistive Switching Characteristics of HfO2-Based Memory Devices on Flexible Plastics. *J. Nanosci. Nanotechno.* **14**, 8191-8195 (2014).
25 Zhang, W. B. *et al.* Thermally-stable resistive switching with a large ON/OFF ratio achieved in poly(triphenylamine). *Chem. Commun.* **50**, 11856-11858 (2014).
26 Heremans, P. *et al.* Polymer and Organic Nonvolatile Memory Devices. *Chem. Mater.* **23**, 341-358 (2011).
27 Chiu, Y. C. *et al.* High performance nonvolatile transistor memories of pentacene using the electrets of star-branched p-type polymers and their donor-acceptor blends. *J. Mater. Chem. C* **2**, 1436-1446 (2014).
28 Baeg, K. J. *et al.* High-Performance Top-Gated Organic Field-Effect Transistor Memory using Electrets for Monolithic Printed Flexible NAND Flash Memory. *Adv. Funct. Mater.* **22**, 2915-2926 (2012).
29 Das, B. C., Pillai, R. G., Wu, Y. L. & McCreery, R. L. Redox-Gated Three-Terminal Organic Memory Devices: Effect of Composition and Environment on Performance. *ACS Appl. Mater. Inter.* **5**, 11052-11058 (2013).
30 Kumar, R., Pillai, R. G., Pekas, N., Wu, Y. L. & McCreery, R. L. Spatially Resolved Raman Spectroelectrochemistry of Solid-State Polythiophene/Viologen Memory Devices. *J. Am. Chem. Soc.* **134**, 14869-14876 (2012).

31 Chiu, Y. C. *et al.* Multilevel nonvolatile transistor memories using a star-shaped poly((4-diphenylamino)benzyl methacrylate) gate electret. *NPG Asia Mater.* **5** (2013).
32 Chou, Y.-H., Chang, H.-C., Liu, C.-L. & Chen, W.-C. Polymeric charge storage electrets for non-volatile organic field effect transistor memory devices. *Polym. Chem.* **6**, 341-352 (2015).
33 Zhou, Y., Han, S. T., Sonar, P. & Roy, V. A. L. Nonvolatile multilevel data storage memory device from controlled ambipolar charge trapping mechanism. *Sci. Rep.* **3** (2013).
34 Orgiu, E. & Samori, P. 25th Anniversary Article: Organic Electronics Marries Photochromism: Generation of Multifunctional Interfaces, Materials, and Devices. *Adv. Mater.* **26**, 1827-1845 (2014).
35 Hayakawa, R., Higashiguchi, K., Matsuda, K., Chikyow, T. & Wakayama, Y. Optically and Electrically Driven Organic Thin Film Transistors with Diarylethene Photochromic Channel Layers. *ACS Appl. Mater. Inter.* **5**, 3625-3630 (2013).
36 Matsui, N. & Tsujioka, T. Carrier mobility of photochromic diarylethene amorphous films. *Org. Electron.* **15**, 2264-2269 (2014).
37 Tsujioka, T., Hamada, Y., Shibata, K., Taniguchi, A. & Fuyuki, T. Nondestructive readout of photochromic optical memory using photocurrent detection. *Appl. Phys. Lett.* **78**, 2282-2284 (2001).
38 Andersson, P., Robinson, N. D. & Berggren, M. Switchable charge traps in polymer diodes. *Adv. Mater.* **17**, 1798-1803 (2005).
39 Raimondo, C. *et al.* Optically switchable organic field-effect transistors based on photoresponsive gold nanoparticles blended with poly(3-hexylthiophene). *Proc. Natl. Acad. Sci. U.S.A.* **109**, 12375-12380 (2012).
40 Taguchi, M., Nakagawa, T., Nakashima, T., Adachi, C. & Kawai, T. Photo-patternable electroluminescence based on one-way photoisomerization reaction of tetraoxidized triangle terarylenes. *Chem. Commun.* **49**, 6373-6375 (2013).
41 Russew, M. M. & Hecht, S. Photoswitches: From Molecules to Materials. *Adv. Mater.* **22**, 3348-3360 (2010).
42 Irie, M., Fulcaminato, T., Matsuda, K. & Kobatake, S. Photochromism of Diarylethene Molecules and Crystals: Memories, Switches, and Actuators. *Chem Rev* **114**, 12174-12277 (2014).
43 Shallcross, R. C., Korner, P. O., Maibach, E., Kohnen, A. & Meerholz, K. Photochromic Diode With a Continuum of Intermediate States: Towards High Density Multilevel Storage. *Adv. Mater.* **25**, 4807-4813 (2013).
44 Korner, P. O., Shallcross, R. C., Maibach, E., Kohnen, A. & Meerholz, K. Optical and electrical multilevel storage in organic memory passive matrix arrays. *Org. Electron.* **15**, 3688-3693 (2014).
45 El Gemayel, M. *et al.* Optically switchable transistors by simple incorporation of photochromic systems into small-molecule semiconducting matrices. *Nat. Commun.* **6** (2015).
46 Borjesson, K. *et al.* Optically switchable transistors comprising a hybrid photochromic molecule/n-type organic active layer. *J. Mater. Chem. C* **3**, 4156-4161 (2015).
47 Orgiu, E. *et al.* Optically switchable transistor via energy-level phototuning in a bicomponent organic semiconductor. *Nat. Chem.* **4**, 675-679 (2012).
48 Chua, L. L. *et al.* General observation of n-type field-effect behaviour in organic semiconductors. *Nature* **434**, 194-199 (2005).